Supporting Information

The thermal and thermoelectric transport properties of SiSb, GeSb and SnSb monolayers

H.H. Huang[a] , Xiaofeng Fan[a,*], David J. Singh[c] and W.T. Zheng[a,b]

a. Key Laboratory of Automobile Materials (Jilin University), Ministry of Education, and College of Materials Science and Engineering, Jilin University, Changchun, 130012, China

b. State Key Laboratory of Automotive Simulation and Control, Jilin University, Changchun 130012, China

c. Department of Physics and Astronomy, University of Missouri, Columbia, Missouri 65211-7010, USA

*, Correspondence and requests for materials should be addressed,

Email: xffan@jlu.edu.cn (X. Fan)

Tel: +86-159-4301-3494

Figure S1

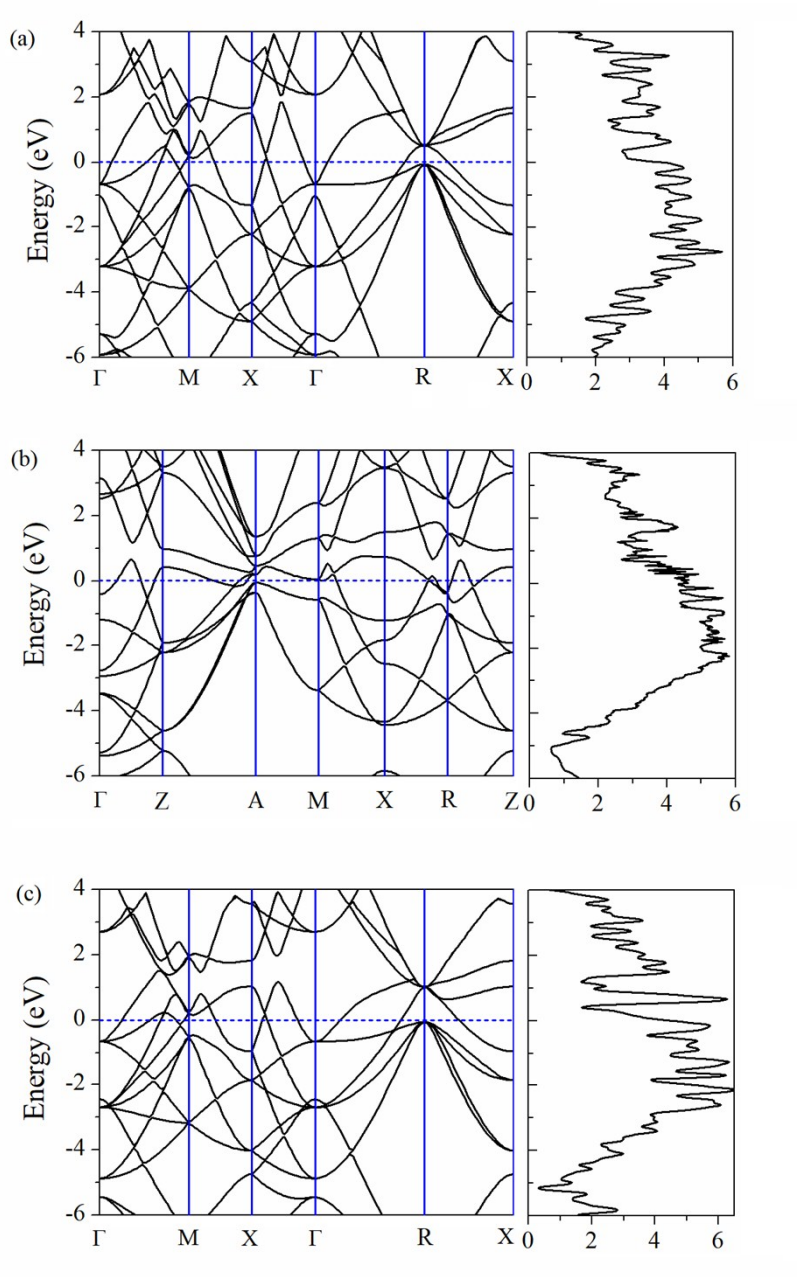

Fig.S1. Band structures and density of states of bulk (a) SiSb, (b) GeSb and (c) SnSb. The dotted line denotes Fermi level. Note that SiSb and SnSb are calculated with NaCl-B1 type structure and GeSb is calculated with tetragonally distorted NaCl-B1 type.

Figure S2

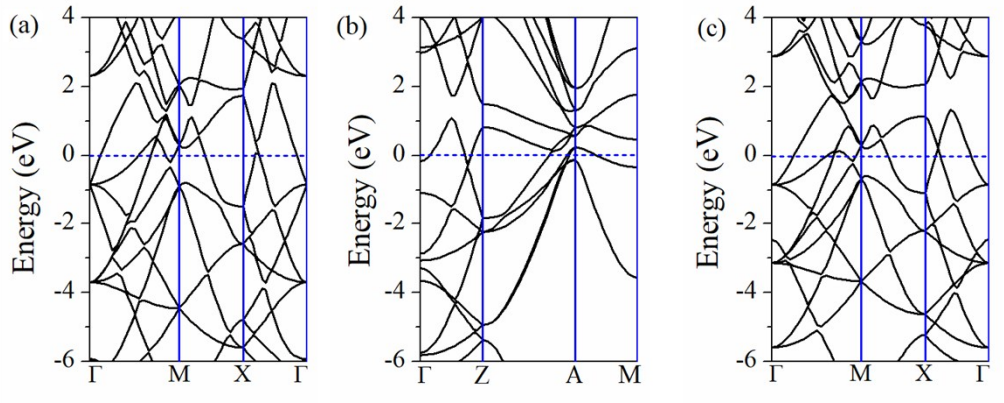

Fig.S2. Band structures for bulk (a) SiSb (b) GeSb and (c) SnSb obtained by using HSE calculation. The dotted line denotes Fermi level.

Figure S3

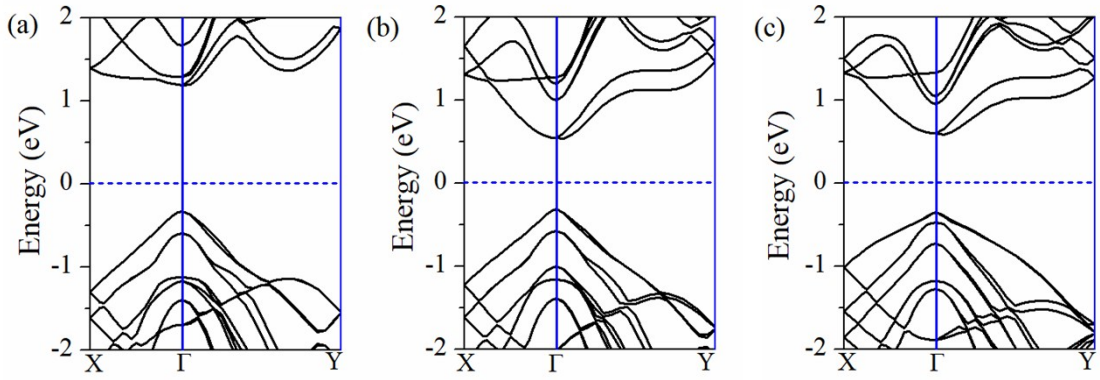

Fig.S3. Band structures for (a) SiSb (b) GeSb and (c) SnSb monolayer obtained by using HSE-SOC calculation. The dotted line denotes Fermi level.

Figure S4

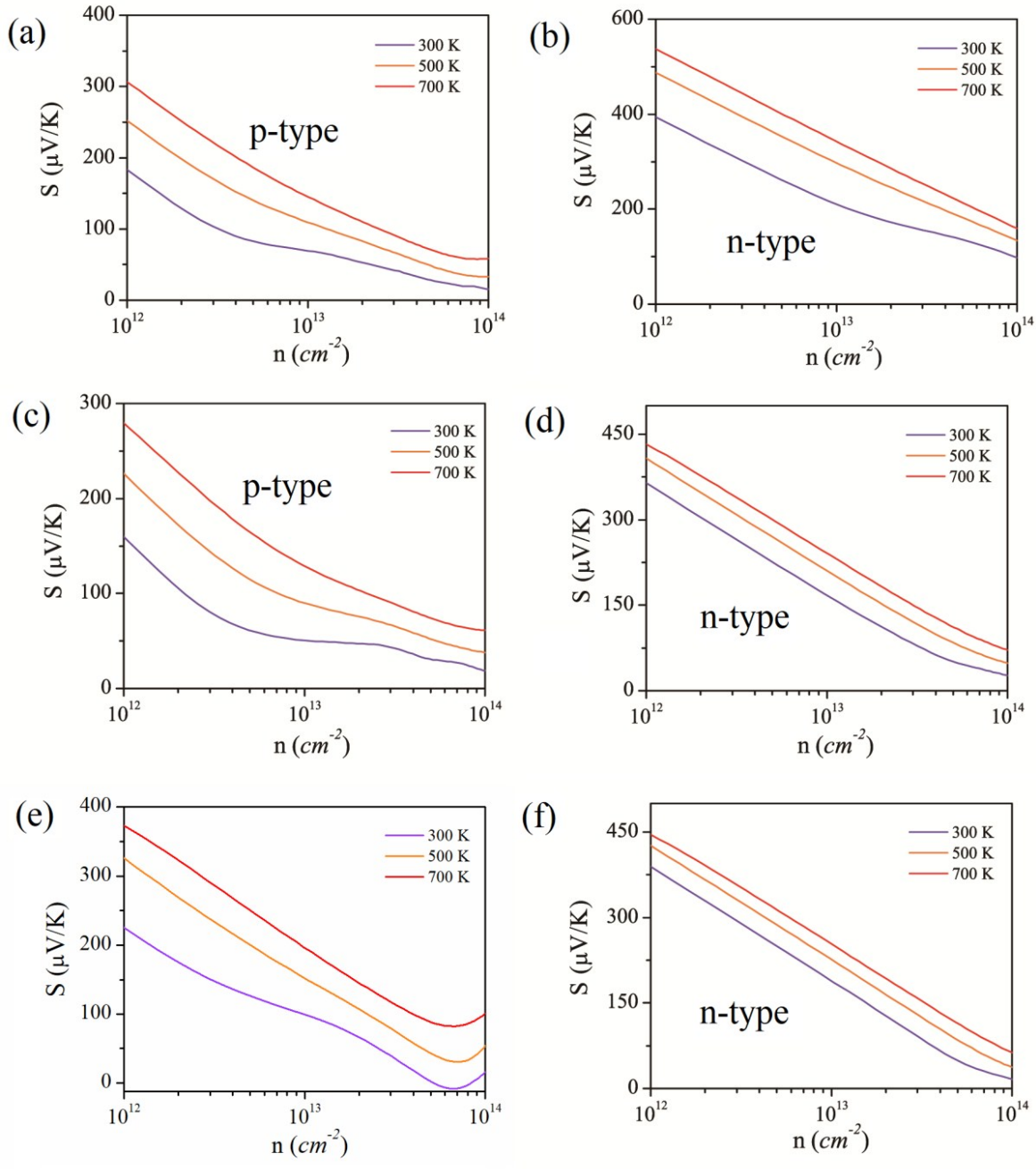

Fig.S4. Seebeck coefficient *S* as a function of carriers' concentration of SiSb, GeSb and SnSb for both (a, c ,e) p-type doing and (b, d, f) n-type doing at 300K, 500K and 700K.

Figure S5

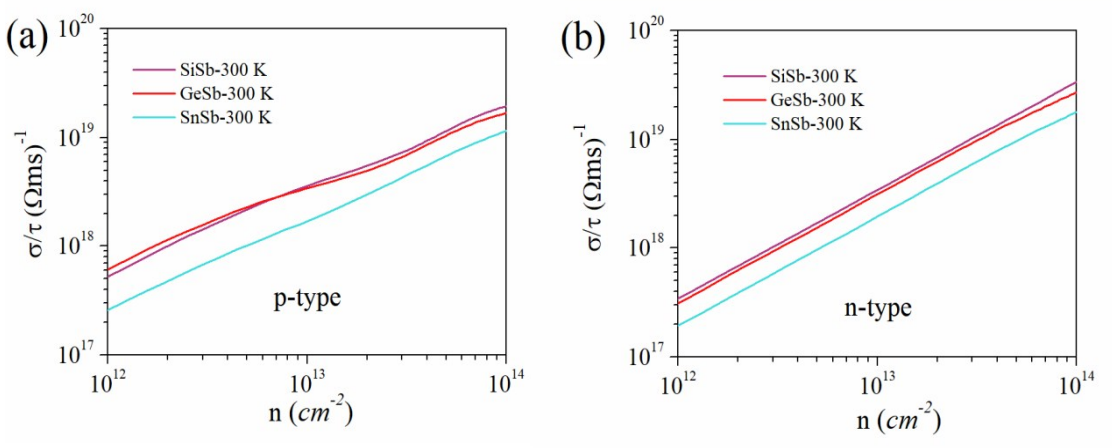

Fig.S5. The reduce conductivity (σ/τ) as a function of carriers' concentration of SiSb, GeSb and SnSb for both (a) p-type and (b) n-type at 300K.

Figure S6

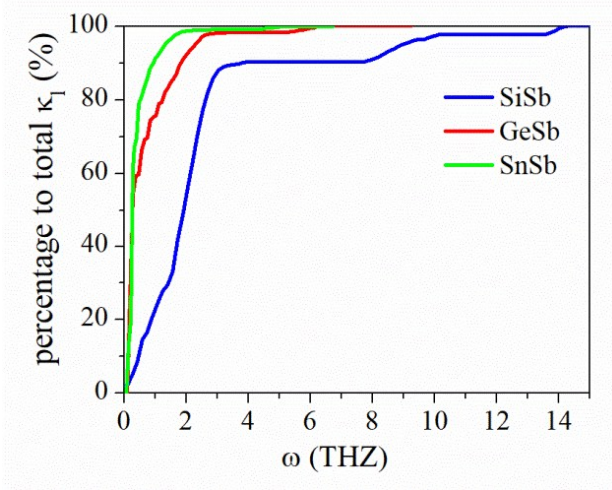

Fig.S6. The percentage of cumulative thermal conductivity to total κ_l as a function of frequency for SiSb, GeSb and SnSb.

Figure S7

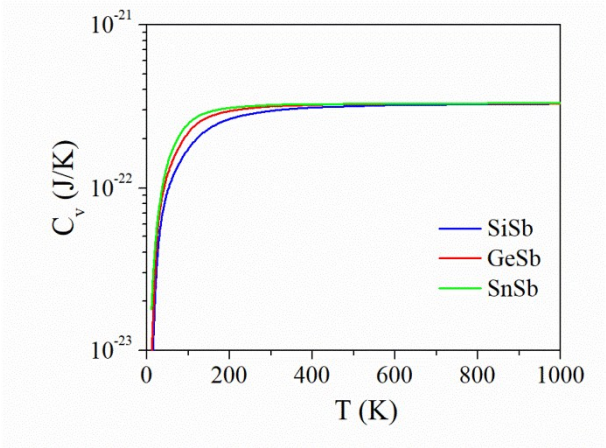

Fig.S7. The specific heat capacity of monolayer SiSb, GeSb and SnSb varies with temperature.

Figure S8

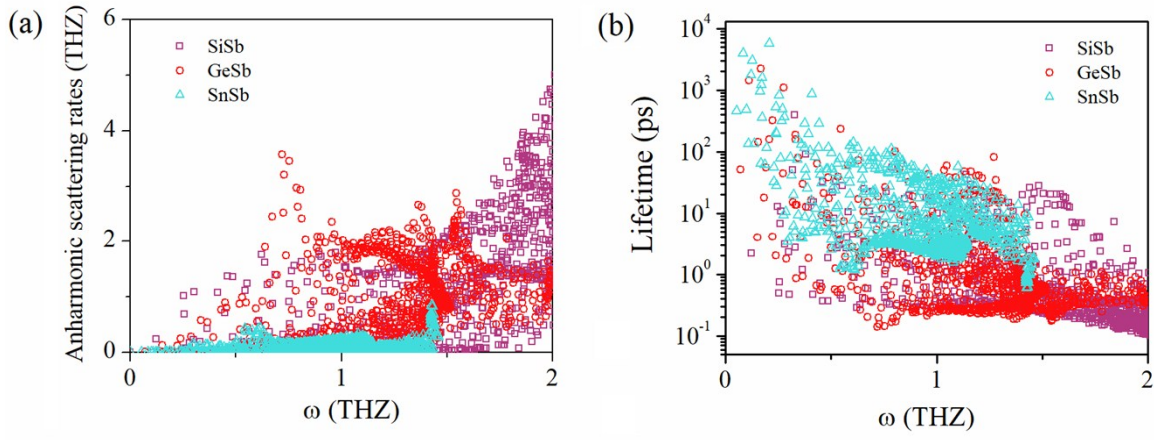

Fig.S8. (a) Anharmonic scattering rates and (b) phonon lifetimes of acoustic phonon modes for SiSb, GeSb and SnSb monolayer at 300K.

Figure S9

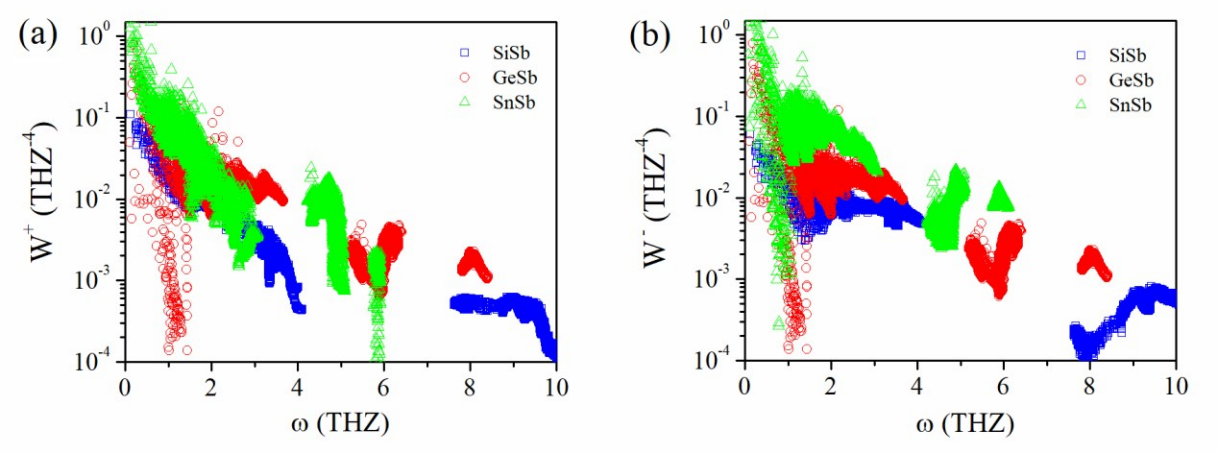

Fig.S9. Scattering phase space of SiSb, GeSb and SnSb monolayer for (a) adsorption processes and (b) emission processes.

Figure S10

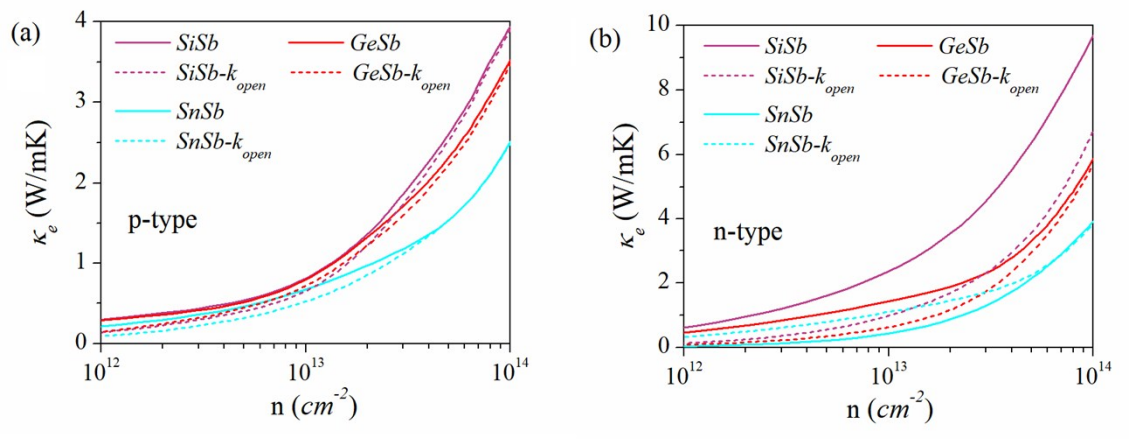

Fig.S10. Electronic thermal conductivity of SiSb, GeSb and SnSb for (a) p-type, (b) n-type at 300K.

Figure S11

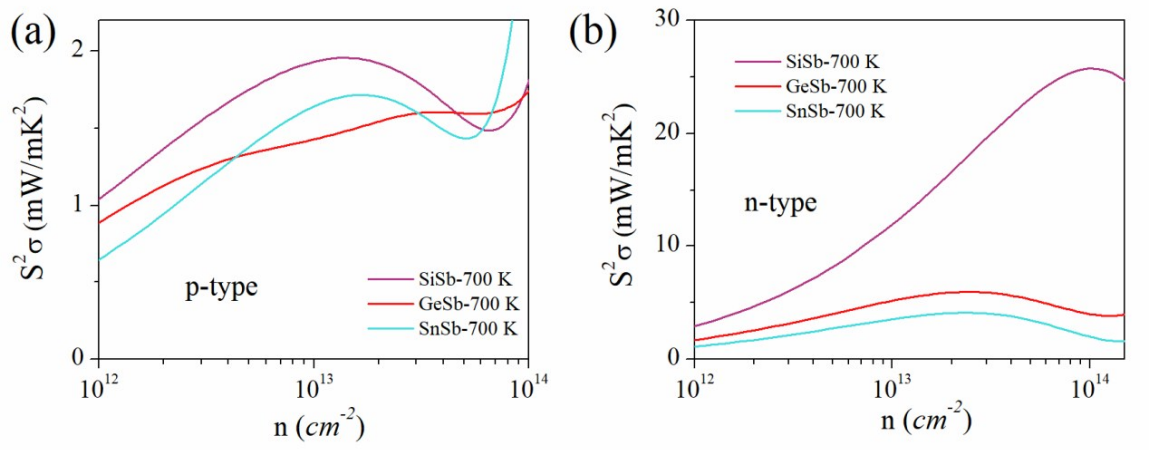

Fig.S11. Power factor of SiSb, GeSb and SnSb as functions of carrier concentration at 700 K for both (a) p-type and (b) n-type.

Figure S12

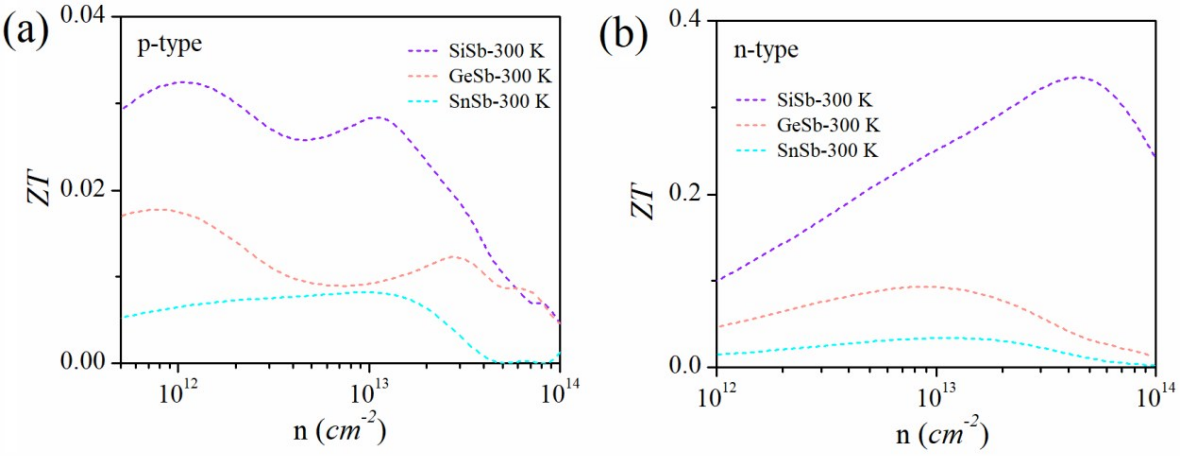

Fig.S12. Calculated *ZT* values of SiSb, GeSb and SnSb as functions of carriers concentration at 300 K for both (a) p-type and (b) n-type.

Figure S13

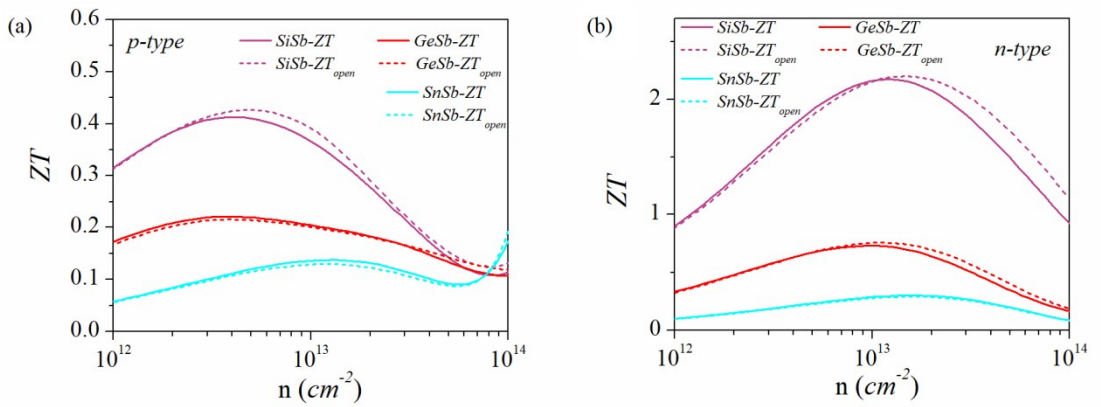

Fig.S13. Calculated ZT and ZT_{open} values of SiSb, GeSb and SnSb as functions of carrier concentration at 700 K for both (a) p-type doping and (b) n-type doping.